Available online at www.sciencedirect.com
ScienceDirect
Catalysis Today 127 (2007) 238–245
CATALYSIS TODAY
www.elsevier.com/locate/cattod

A kinetic study of methane and carbon dioxide interconversion over 0.5%Pt/$SrTiO_3$ catalysts

A. Topalidis [a], D.E. Petrakis [a], A. Ladavos [b], L. Loukatzikou [a], P.J. Pomonis [a,*]

[a] *Department of Chemistry, University of Ioannina, Ioannina 45110, Greece*
[b] *School of Natural Resourses and Entreprise Management, University of Ioannina, Agrinio 30100, Greece*

Available online 31 May 2007

Abstract

The kinetics of interconversion of methane with carbon dioxide was studied over a 0.5%Pt/$SrTiO_3$ solid catalyst in the temperature range 813–893 K and partial pressure range $0.083 < P_{CH_4}, P_{CO_2} < 0.667$. The fitting of the experimental data for the rate of methane conversion, R_{CH_4}, using the empirical equation $R_{CH_4} = k_1(P_{CH_4})^m(P_{CO_2})^n$ showed that both reaction orders n and m are steady and obtain values equal to $m \approx 1$ and $n \approx 0$. The results are explained using Langmuir–Hinshelwood kinetics with the *reactants adsorbed on distinct and discreet active sites* of the solids, namely the methane is weakly adsorbed on the metallic phase and the carbon dioxide is strongly adsorbed on the oxidic phase of the catalyst. The apparent activation energy for the reforming of methane was estimated to be ~123 kJ mol^{-1}.

The rate of conversion of the carbon dioxide, R_{CO_2}, was also fitted using a similar empirical equation $R_{CO_2} = k_2(P_{CH_4})^m(P_{CO_2})^n$. The results indicate that there is a positive but variable dependence on both reaction orders which increases in the temperature range 813–893 K from $m \approx 0.0$ to $m \approx 0.30$ and from $n \approx 0.3$ to $n \approx 0.6$. This variation is attributed to the variable participation of the rate of the reverse water gas shift reaction, $R_{rwgs,}$ to the overall rate R_{CO_2} of CO_2 conversion. The dependence of R_{rwgs} on the partial pressure of CO_2 appears similar to that of R_{CH_4} on the same reactant but shows strong inhibition by the reaction products. The results are discussed using Langmuir–Hinshelwood kinetics with the reactants and products adsorbed *competitively on similar active sites* of the catalyst.

Keywords: Dry reforming of methane; Kinetics of dry reforming; Reverse water gas shift reaction; Pt/$SrTiO_3$ catalysts

1. Introduction

Methane exists in very large amounts in nature while carbon dioxide is produced also in huge quantities by various industrial activities. Since both gases are relatively inexpensive, their inter-conversion to higher value compounds is of high interest. Indeed the reforming of CH_4 by CO_2 was explored by Fischer and Tropsch already in 1928 [1]. The main route is towards synthesis gas with ratio $H_2/CO \sim 1$, which is more suitable for methanol and other Fischer–Tropsch syntheses, compared to the steam reforming of methane which provides synthesis gas with ratio $H_2/CO \sim 3$ [2–12]. The interest for this reaction has been increased during the last years due to both environmental (green house effects of carbon dioxide) and energy reasons (increased availability and use of natural gas). Another specific reason for the increased interest for this technology is that CH_4 and CO_2 gases are the main constituents of biogas produced extensively by various anaerobic biological waste treatments [13,14] which is often of pure quality but its valorization can be enhanced through this process.

The catalysts employed for this reaction are of dual nature. Namely they are consisted of a metal, either noble like Ru, Rh, Pt, Pd, or transition one like Ni, Co, Cu and an oxidic phase like SiO_2, Al_2O_3, MgO, BaO, CeO_2, La_2O_3, TiO_2 and ZrO_2 [3]. The combination of those components leads to various dual catalysts but it has been recognized that the Ni and Pt based ones provide the best activity [8–11]. The most important difference between catalysts based on those two metals is the resulting carbon deposition, either amorphous or in the the form of nanofibers, which is higher on Ni and for this reason it appears as more active.

The reaction mechanism on such catalytic solids appear often diverse but there is a general consensus that CH_4 and CO_2 are adsorbed in dissociated form on the metallic and the oxidic

* Corresponding author. Tel.: +30 2651098350.
E-mail address: ppomonis@cc.uoi.gr (P.J. Pomonis).

0920-5861/$ – see front matter © 2007 Elsevier B.V. All rights reserved.
doi:10.1016/j.cattod.2007.04.015

catalyst components [3,10]. Unfortunately the resulting equations describing the kinetics appear often very diverse [3]. Such kinetics are almost always referred to the rate of methane conversion and rarely to the conversion rate of carbon dioxide. The reason is that this last reactant participates in two parallel reactions, the dry conversion of methane as well as the reverse water gas shift reaction (rwgs) which has not been studied extensively itself but usually in conjunction with the forward water gas shift reaction [15–19]. The purpose of the present work is to examine the interconversion of methane and carbon dioxide and to propose kinetic equations for *both* reactions contributing to their disappearence. The catalyst employed was Pt supported on a perovskite solid $SrTiO_3$. This solid can be considered as the first member of the substituted series Pt/Sr_{1-x} $La_xTiO_{3\pm\delta}$ which is the subject of a more extensive study [20]. The choice of perovskite as support stems from the fact that in the past noble metal supported on similar mixed valence oxidic solids have shown superior catalytic activity for reactions like the lean de-NO_x and $NO + CH_4 + O_2$ conversion [21,22].

2. Experimental

2.1. Preparation and characterization of the of the catalyst

The sample $0.5\%Pt/SrTiO_3$ was prepared as follows: the calculated amounts of $Sr(NO_3)_2$ and $Ti[O(CH_2)_3CH_3]_4$ were dissolved in distilled water and precipitation took place with NH_3 0.1 M at pH 7.0. The obtained gel was then dried at 373 K, fired at 1073 K for 6 h and grounded in an agate mortar. The addition of 0.5% Pt took place by the dry impregnation method using suitable portions of a solution of 0.01M H_2PtCl_6 and calcining at 873 K C for 4 h.

The calcined materials were characterized by XRD for their crystal structure in a Bruker Advance P8 system using Cu Kα radiation (λ = 1.5418) with step 0.02° per second. The X-ray diffractogram is shown in Fig. 1.

The solid catalyst was also photographed for its morphology by scanning electron microscopy (SEM) in a Jeol JSM 5600 system operating at 20 kV. The corresponding microphotographs are shown in Fig. 2.

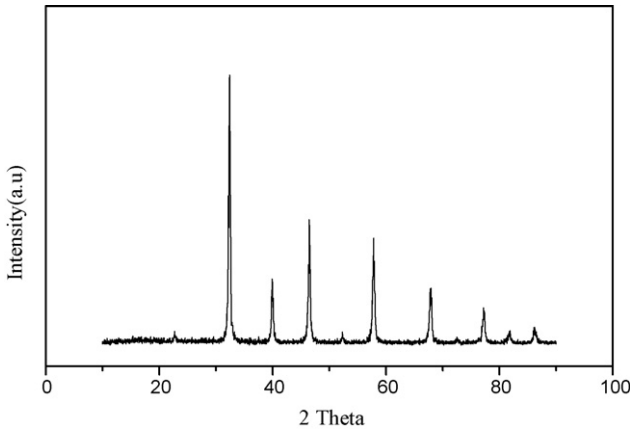

Fig. 1. X-ray diffractogram analysis of the samples $0.5\%Pt/SrTiO_3$. All the peaks correspond to perovskites structure.

The solids, after the catalytic tests described next, were examined in a thermogravimetric system in order to check the possible accumulation of carbon in them, by detecting simultaneously the TG and the DTA signals. The study took place in a STA 449C Jupiter system by Netzsch under air flow (30 ml/min) in the temperature range $300\ K < T < 1273\ K$ and a heating rate of 10°/min. The results are shown in Fig. 3.

The surface area of the catalyst was checked by the BET method and it was low ∼12 m^2/g as expected for such materials without internal porosity.

2.2. Catalytic experiments

The catalytic experiments took place in a bench scale plug flow reactor (PFR) containing 200 mg of solid in the catalytic bed. The height of the catalyst bed was about 3 mm and the size of the catalyst particles in the range of 1–10 μm. The reactor was made of quartz with 1 cm i.d. The catalyst zone of the reactor was heated by a tubular furnace with a suitable controller by SUR Berlin connected to a thermocouple in touch with external surface of the silicate reactor. The catalyst was initially reduced under flow of 15 cc H_2/min for 1 h at 773 K (500 °C) followed by striping under flow of 20 cc He/min for 30 min at 1023 K (750 °C). The feed flow in the reactor was 60 cc/min made up of $He:CH_4:CO_2 = x:y:z$ and adjusted by MKS 247 mass flow controllers. The values of the x, y, z in the various experiments are cited in Table 1. Each experiment took place at five different temperatures 813, 833, 853, 873 and 893 K. The analyses of reactants and products were carried out by sampling 1cc of gases, via a suitably connected loop of a 10 port valve, to a Shimadzu 15 A GC, equipped with a TCD, with He as carrier gas. The analytical column in the GC was Carboxen 1000 (Supelco) and the obtained signals were stored and processed in a PC equipped with a suitable software for data acquisition. The hydrogen was not analyzed in the system used but the production of water was reproducible. The degree of conversion x% of both methane and carbon dioxide in the experiments was kept below 15%. From these values, and the corresponding feeds, the reaction rates of methane R_{CH_4} and carbon dioxide R_{CO_2} conversion were estimated in $\mu mol\ s^{-1}\ g^{-1}$.

3. Results

The X-ray diffraction data in Fig. 1 were compared to the standard JCPDS reference reflexes from the Data Bank of the Bruker Advance P8 instrument. From the comparison it is clear that the only peaks were those of perovskite $SrTiO_3$ and the catalyst possesses the corresponding structure. The size of crystallites estimated from the Scherrer relationship was found around 200 nm (0.2 μm). No peaks attributable to Pt could be detected, which means that any crystallites of the metal were very small (probably less than 5 nm) and in high dispersion on the perovskite matrix.

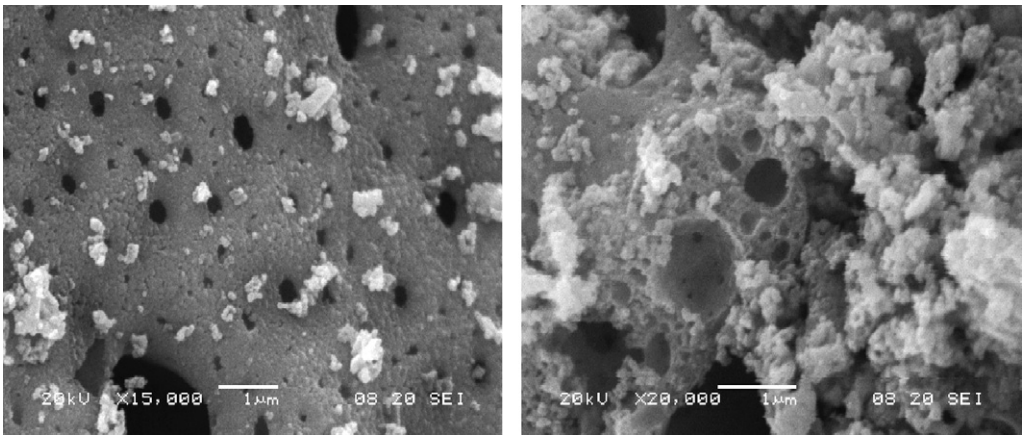

Fig. 2. Typical SEM microphotographs of the catalysts.

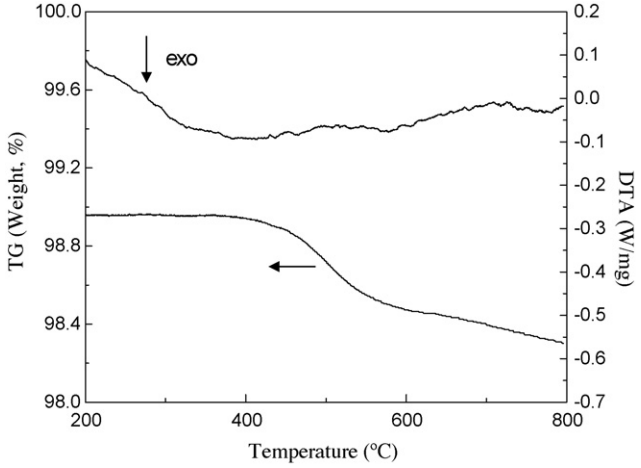

Fig. 3. Thermogravimetric (TG) and Differencial Thermal Analysis (DTA) signals of the catalysts after the catalytic tests.

The SEM microphotographs in Fig. 2 reveal a uniform nanostructured textural background with particles of regular size in the range of 0.2 μm, in line with that calculated via the Scherrer relationship (see left hand photo in Fig. 2). This uniform background is perforated by macropores due to the sol–gel preparation method. The Energy Dispersive Spectra (EDS) analysis of the sample surface indicated that the surface is depleted of Sr and Ti by an amount of 10 and 30%, respectively, enriched in oxygen by almost 50% while the detected Pt on the surface was only ∼20% of the nominal amount used in the synthesis. This indicates that the almost ∼80% of the Pt is trapped inside the ceramic matrix and probably not available for surface reaction.

From the Thermogravimetric (TG) and Differencial Thermal Analysis (DTA) of the used samples after the catalytic tests, which are shown in Fig. 3, it is observed that the weight loss in the temperature range 400–600 °C, due to the combustion of the carbon deposited on the catalyst, is about ≈0.6%. In other words the possible amount of carbon deposited on the solid was of the same order as the supported Pt, probably in the form of a few monolayers. The TG/DTA analysis of the fresh sample (not shown here, see Supplementary Information) did not indicated any specific weight loss at this temperature range but a continuous water loss and/or dehydroxylation at $T > 373$ K.

The reaction rates for the conversion of methane R_{CH_4} and carbon dioxide R_{CO_2} calculated in μmol s^{-1} g^{-1} are shown in Figs. 4 and 5 in the form $R_{CH_4} = f(P_{CH_4})$, $R_{CH_4} = f(P_{CO_2})$ and $R_{CO_2} = f(P_{CH_4})$, $R_{CO_2} = f(P_{CO_2})$.

The points in these figures correspond to the experimental results and the lines are the fittings using the semi-empirical formulae:

$$R_{CH_4} = k_1 (P_{CH_4})^{m_1} (P_{CO_2})^{n_1} \quad (1)$$

$$R_{CO_2} = k_2 (P_{CH_4})^{m_2} (P_{CO_2})^{n_2} \quad (2)$$

where k_1, m_1, n_1, k_2, m_2, n_2 are parameters to be determined. Their values estimated from the fitting according to Eqs. (1) and (2) are cited in Table 2.

Table 1
Partial pressures of methane (P_{CH_4}) and carbon dioxide (P_{CO_2}) used for the determination of kinetics of their interconversion

P_{CH_4} (atm)	0.333	0.333	0.333	0.333	0.333	0.333	0.333	0.333	0.333
P_{CO_2} (atm)	0.083	0.125	0.167	0.208	0.250	0.292	0.333	0.500	0.667
P_{He} (atm)	0.584	0.542	0.500	0.459	0.417	0.375	0.333	0.167	0.000
P_{CH_4} (atm)	0.083	0.125	0.167	0.208	0.250	0.292	0.333	0.500	0.667
P_{CO_2} (atm)	0.333	0.333	0.333	0.333	0.333	0.333	0.333	0.333	0.333
P_{He} (atm)	0.584	0.542	0.500	0.459	0.417	0.375	0.333	0.167	0.000

The balance is Helium (P_{He}). For each pair of pressures (P_{CH_4}, P_{CO_2}) the conversion was examined at 540, 560, 580, 600 and 620 °C.

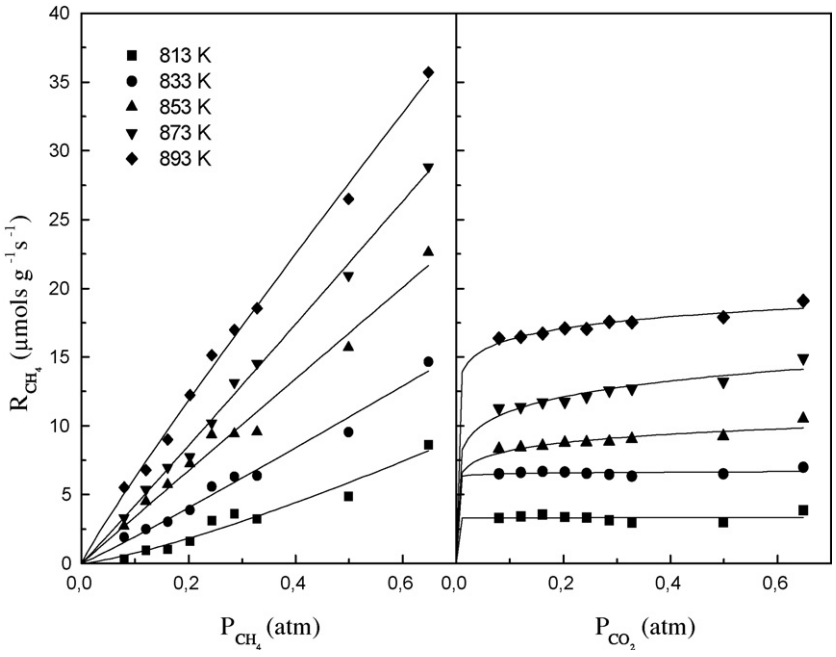

Fig. 4. Variation of the reaction rates for the conversion of methane R_{CH_4} as a function of the partial pressures of methane P_{CH_4} and of carbon dioxide P_{CO_2} at the indicated temperatures. The points are experimental data. The lines are the fitting using the Eqs. (3) and (5).

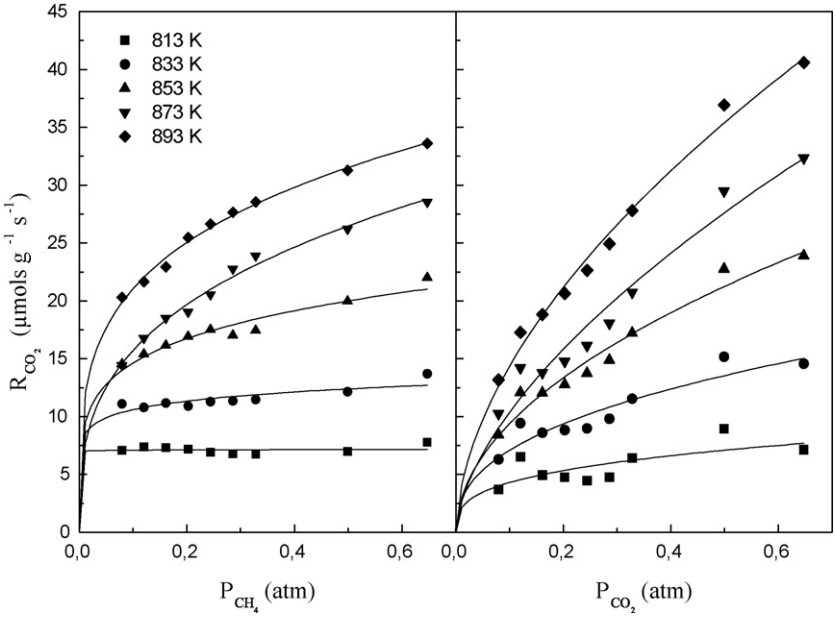

Fig. 5. Variation of the reaction rates for the conversion of carbon dioxide R_{CO_2} as a function of the partial pressures of methane P_{CH_4} and of carbon dioxide P_{CO_2} at the indicated temperatures. The points are the experimental data. The lines are the fitting using the Eqs. (4) and (6).

4. Discussion

The dry catalytic conversion of methane proceeds according to reaction

$$CH_4 + CO_2 \rightarrow 2CO + 2H_2 \quad (3)$$

On top of reaction (3) the reverse water gas shift (rwgs) reaction takes place to an extend depended on the solid catalyst and the reaction conditions

$$CO_2 + H_2 \rightarrow CO + H_2O \quad (4)$$

If the feeding of the reactor is (moles CH_4: moles CO_2) = 1:N, the converted moles of CH_4 and CO_2 in reaction (3) are $N_{CH_4} = N_{CO_2} = N_I$ and the converted moles of H_2 in reaction (4) are $N_{H_2} = N_{II}$, then during each time the combined conversion will be described by the following stoichiometry:

$$(1 - N_I)CH_4 + (N - N_I - N_{II})CO_2 \rightarrow (2N_I + N_{II})CO + (2N_I - N_{II})H_2 + (N_{II})H_2O \quad (5)$$

This means that CO is always *in excess* of H_2 and this difference increases with the extend of rwgs reaction. We shall

Table 2
The parameters k_1–m_1–n_1 and k_2–m_2–n_2 used for the fitting of Eqs. (1) and (2) to the experimental points in Figs. 4 and 5

T (K)	$R_{CH_4} = k_1(P_{CH_4})^{m_1}(P_{CO_2})^{n_1}$			$R_{CO_2} = k_2(P_{CH_4})^{m_2}(P_{CO_2})^{n_2}$		
	k_1	m_1	n_1	k_2	m_2	n_2
813	14.1	1.28	0.01	9.5	0.01	0.31
833	22.0	1.05	0.01	20.3	0.10	0.40
853	34.1	0.99	0.10	38.7	0.19	0.51
873	48.8	1.02	0.13	62.6	0.32	0.61
893	54.9	0.92	0.07	69.3	0.25	0.56

discuss first the kinetics of methane conversion, which proceeds according to Eq. (3), and then the kinetics of carbon dioxide conversion, which proceeds according to Eqs. (3) and (4).

4.1. The kinetics for the conversion of CH_4

All the catalysts proposed and developed for the dry conversion of CH_4 by CO_2 are made up of two components: A metallic one like Ni, Ru, Rh, Pd, Ir, Pt and Co, and an oxidic part like SiO_2, Al_2O_3, MgO, TiO_2, CaO, CeO_2, ZrO_2 and La_2O_3 [3]. Those two components are responsible for two distinct operations during adsorption, namely the metal adsorbs and activates the methane while the basic oxide adsorbs and activates the slightly acidic carbon dioxide [3,10]. Thus, the crucial assumptions underlying the conversion of methane are the following [3,10].

(i) Methane is adsorbed only on the metal in a dissociate form producing hydrogen and hydro-carbonate species CH_x where the value of x is in the range $0 \leq x < 4$ and depends on the metal substrate and the temperature. Most often the value of x is around zero, meaning that actually carbon is formed on the metal surface.

$$CH_4 + ME \rightarrow CH_4 \ldots ME \quad (6)$$

$$CH_4 \ldots ME + 4ME \rightarrow C \ldots ME + 4(ME \ldots H) \quad (7)$$

where ME is the metal site on which adsorption and dissociation of methane takes place. The species of carbon and hydrogen are attached to the metal sites and this is a crucial point influencing the kinetics of the reverse water gas shift reaction discussed next. The large majority of the adsorbed hydrogen species are then recombined producing hydrogen molecules desorbed in the gaseous phase

$$2(ME \ldots H) \rightarrow 2ME + H_2 \quad (8)$$

Nevertheless some of the adsorbed hydrogen species, always on the metallic sites, might not be desorbed but find some neighboring adsorbed CO_2 species and react with them towards CO and H_2O, e.g. the rwgs reaction.

(ii) Carbon dioxide is adsorbed on the basic metal oxidic component of the catalyst forming some kind of oxycarbonates species. The adsorption takes place in dissociate form

$$CO_2 + MO \rightarrow MO \ldots CO_2 \quad (9)$$

$$CO_2 + 2MO \rightarrow MO \ldots CO + MO \ldots O \quad (10)$$

where MO is the metal oxide site on which adsorption of carbon dioxide, and/or oxygen takes, place.

(iii) The oxycarbonates species react with the carbon deposits forming carbon monoxide according to the following possible surface reactions

$$MO \ldots CO_2 + ME \ldots CH_4 \rightarrow 2CO + 2H_2 + MO + ME \quad (11)$$

$$MO \ldots CO_2 + C \ldots ME \rightarrow 2CO + MO + ME \quad (12)$$

$$MO \ldots O + C \ldots ME \rightarrow CO + MO + ME \quad (13)$$

The above point (iii) implies that the reaction takes place at the interface of the adsorbing metallic ME and metal oxide MO sites. But of course not all the adsorbing metallic ME and metal oxide MO sites are in close proximity to allow the main and overall reaction (11), or the subreactions (12) and/or (13), although allowing reactions (6) + (7) and (9) + (10). Considering that the fractions of the adsorbing metallic ME and metal oxide MO sites which are in close proximity as to allow the main and overall reaction (11) are θ_{ME} and θ_{MO}, respectively, and applying standard Lamgmuirian kinetics with *the adsorption taking place on distinct and discreet sites* we obtain for the rate of methane disappearance

$$R_{CH_4} = k\theta_{ME}\theta_{MO} = k\left[\frac{K_{CH_4}P_{CH_4}}{1 + \sum K_I P_I}\right]\left[\frac{K_{CO_2}P_{CO_2}}{1 + \sum K_J P_J}\right] \quad (14)$$

where I are all the species adsorbed on the ME and J all the species adsorbed on the MO *at the interfaces ME ↔ MO as this is the crucial niche* where the adsorption of I's and J's would have any effect on the process. This practically implies that I = CH_4, CO, H_2 and H_2O and that J = CO_2 CO, H_2 and H_2O. Of those species H_2, as well as CH_4, are known to be adsorbed very weakly on both metal and non metal surfaces, so the terms $(K_{H_2}P_{H_2})$ and $(K_{CH_4}P_{CH_4})$ are expected to be small compared to unity because the adsorption term K_{H_2} and K_{CH_4} are small. On the other hand if the degrees of conversion $(1 - N_I)$ of methane and $(N - N_I)/N$ of carbon dioxide (see Eq. (5)) are small, let us say less than 10%, and also the reverse water gas shift reaction (4) proceeds to a small degree to the right, i.e. N_{II} is small compared to N_I, then the terms $(K_{CO}P_{CO})$ and $(K_{H_2O}P_{H_2O})$ will be also small compared to unity because the partial pressure terms P_{CO} and P_{H_2O} will be small. Under those conditions, Eq. (14) is reduced to

$$R_{CH_4} = k[K_{CH_4}P_{CH_4}]^1\left[\frac{K_{CO_2}P_{CO_2}}{1 + K_{CO_2}P_{CO_2}}\right] \quad (15)$$

which for $1 \ll (K_{CO_2}P_{CO_2})$ provides

$$R_{CH_4} = k[K_{CH_4}P_{CH_4}]^{\sim 1}[K_{CO_2}P_{CO_2}]^{\sim 0} \quad (16)$$

Eq. (16), derived on semi-theoretical ground, is favorably compared to the semi-empirical relationship (1) used for the fitting of the experimental results in Fig. 4. The values of the parameters k_1–m_1–n_1 used for the fitting of Eq. (1) are collected

in Table 2. The fitting is very good indeed and the averaged values of exponents are $m_1 = 1.05 \pm 0.10$ and $n_1 = 0.06 \pm 0.05$ which is practically similar to the unity and the zero values predicted by theory in Eq. (16).

The apparent activation energy E_{app} of methane conversion according to reaction (3) can be estimated from the Arrhenius plot of the form $\ln(k_1) = f\,(1000/T)$ which is shown in Fig. 6. According to the above discussion $k_1 = kK_{CH_4}$ and therefore $E_{app} = E_{true} - \lambda_{CH_4}$ where the last term corresponds the heat of methane adsorption. The value of E_{app} was estimated to be around 123 kJ/mol which is favourably compared to values from previous studies [3,10,12]. The point corresponding to the higher temperature in the Arrhenius plot in Fig. 6 is obviously out of trend due to diffusion limitations. It is not clear if those limitations are external or internal ones due to the porous features of the catalyst seen in the SEM microphotographs (see Fig. 2).

The assumptions underlying the derivation of kinetic Eqs. (15) and (16) are semi-theoretical but based on standard kinetic principles. The final result tallies remarkably with the kinetic equation estimated experimentally by Bradford and Vannice on different catalysts like Ni/MgO, Ni/TiO_2 and Pt/TiO_2 [3]. In those cases the general equation proposed has the form

$$R_{CH_4} = \frac{K_1 P_{CH_4} P_{CO_2}}{K_2 P_{CO} P_{H_2} + K_3 P_{CO_2} + K_4 P_{CH_4} P_{CO_2}} \tag{17}$$

Substitution of the values for K_1, K_2, K_3 and K_4 provided by the authors [3] in Eq. (17) leads to the result that the only important term in the denominator is actually the $K_3 P_{CO_2}$ which means that this is practically similar to Eq. (16). This means that the applicability of the *distinct and discreet active site model*, stemming from crucial assumptions (i), (ii) and (iii) underlying the conversion of methane [3,10], is a powerful tool for the description of kinetics of dry methane conversion on seemingly dissimilar catalysts.

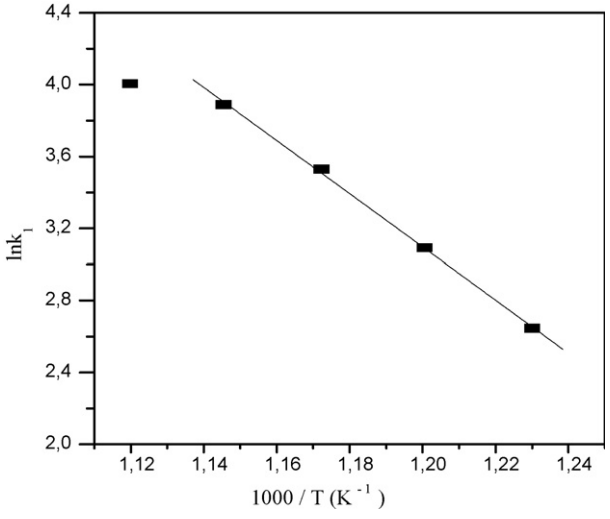

Fig. 6. Arrhenius plot $\ln k_1 = f\,(1000/T)$ for the estimation of the apparent activation energy ($E_{app} \approx 123$ kJ/mol) of methane conversion.

4.2. The kinetics of CO_2 conversion and of rwgs reaction

While methane is converted according to reaction (3), carbon dioxide is converted according to reactions (3) and (4). So the total reaction rate R_{CO_2} should be the sum of two parallel reactions rates, that of methane conversion R_{CH_4} (3) *plus* the rate of the reverse water gas shift reaction, R_{rwgs} (4).

$$R_{CO_2} = R_{CH_4} + R_{rwgs} \tag{18}$$

The phenomenological fitting of the variation of R_{CO_2} to the partial pressures of CH_4 and CO_2 according to Eq. (2) is shown in Fig. 5. Although the fitting appears very satisfactory indeed, the physical insight behind these results is poor since the exponents m_2 and n_2 (see Eq. (2) and Table 2) used for the fitting are not constant but show a temperature dependence. This is due to the fact that the conversion follows two parallel paths and a single power law expression is impossible to describe the final complex outcome. The first rate component R_{CH_4} was analyzed in the previous section. The second rate component R_{rwgs} can be estimated from the difference

$$R_{rwgs} = R_{CO_2} - R_{CH_4} \tag{19}$$

using the experimental data from Figs. 4 and 5. The results are depicted as points in Fig. 7.

The rate R_{rwgs} of the reverse water gas shift reaction and its dependence on the partial pressure of CO_2 and CH_4 has not been studied often itself but usually in connection to the rate R_{wgs} of water gas shift reaction which is related to the methanol synthesis [15,16]. In a few cases [12,13] where the rwgs reaction was studied itself and not in the context of the wgs reaction [17–19], it was indicated that this is a complex process. In the present catalytic tests, there is no hydrogen as primary reactant but produced by the conversion of methane according to reaction (3). Therefore, $P_{H_2} = 2xP_{CH_4}$ where x is the degree of methane conversion. Such dependence is valid only at very low methane conversion. Apart from hydrogen, carbon monoxide CO is also produced in the same ammount by reaction (3) and $P_{CO} = 2xP_{CH_4}$. More importance is the fact that the partial pressure of H_2 decreases very fast with the progress of rwgs reaction while that of CO increases while water is also produced by the same reaction (4) but to a much smaller extend. To cite some values estimated from the stoichiometric Eq. (5), if $N = 1$, $N_I = 0.15$ and $N_{II} = 0.3N_I$ then $P_{CO} : P_{H_2} : P_{H_2O} = 7 : 5 : 1$, in other words CO and H_2 dominate and CO is in excess.

The functional dependence $R_{rwgs} = f(P_{CH_4})$ exhibits an early maximum and then drops very fast which is an unmistaken indication of strong inhibition by the products CO, H_2 and H_2O. The first of them is a notorious surface poison existing in considerable amounts in the reaction mixture, the second is not strongly adsorbed but exists also in large amounts in the mixture while the water is strongly adsorbed but its partial pressure is small. On the other hand, the functional dependence $R_{rwgs} = f(P_{CO_2})$ shows a almost linear form and middle

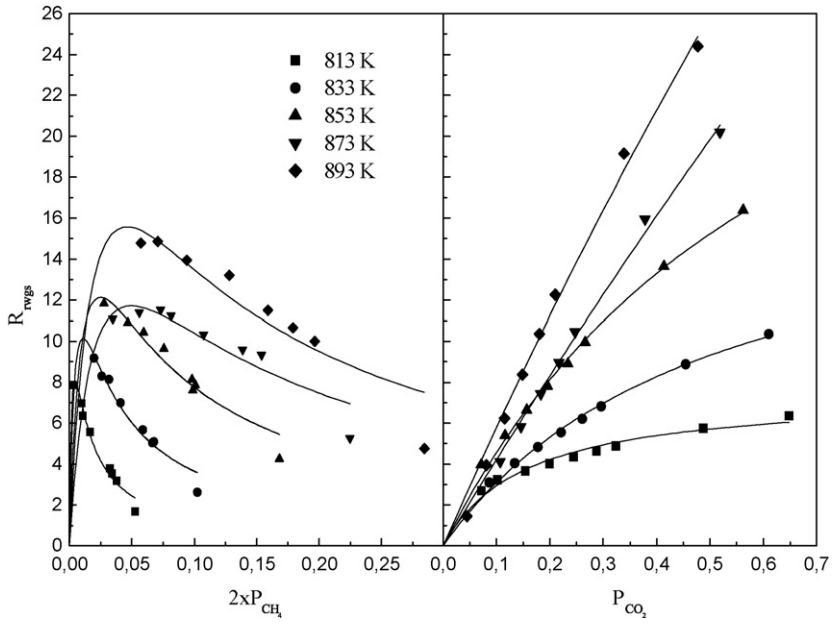

Fig. 7. Variation of the reaction rate of the reverse water gas shift reaction R_{rwgs} as a function of the partial pressures of methane P_{CH_4} and of carbon dioxide P_{CO_2} at the indicated temperatures. The points are the experimental data. The lines are the fitting using the Eqs. (21) and (22).

inhibition effects. These results can be fitted using the equations

$$R_{rwgs} \approx \frac{k_1(2xP_{CH_4})}{[1 + K(2xP_{CH_4})]^2} \quad (20)$$

$$R_{rwgs} \approx \frac{k_2 P_{CO_2}}{[1 + K_{CO_2} P_{CO_2}]} \quad (21)$$

The calculated values for $k_1 - K$ as well as $k_2 - K_{CO_2}$ are cited in Table 3 and the fitting, shown in Fig. 7, is quite satisfactory. So the overall equation describing the rwgs reaction rate has the form

$$R_{rwgs} = k\left\{\frac{k_1(2xP_{CH_4})}{[1 + K_{H_2}(2xP_{CH_4})]^2}\right\}\left\{\frac{k_2 P_{CO_2}}{[1 + K_{CO_2} P_{CO_2}]}\right\} \quad (22)$$

which for P_{CO_2} = constant yields Eq. (20) while for $(2xP_{CH_4})$ = constant provides Eq. (21) and k is a proportionality constant.

The squared denominator in Eqs. (20) and (22) indicates strong inhibition by the CO species and/or by the H_2O molecules. It has been suggested in the past [17] that the forward and the reversed wgs reactions are practically controlled by the formation and decomposition of some relatively stable formate-type intermediate species depicted as $CO^{\bullet}H_2O$ or $H_2O^{\bullet}CO$. The fraction $\theta_{CO^{\bullet}H_2O}$ of the surface, (probably at the interface metal-oxide), covered by these intermediate species should be proportional to the rate of their formation and can be described by the following Langmuir–Hinshelwood type relationship describing *competitive adsorption on similar sites*.

$$\theta_{CO^{\bullet}H_2O} \approx R_{CO^{\bullet}H_2O} = k\theta_{H_2O}\theta_{CO} = \frac{k[K_{CO}P_{CO}K_{H_2O}P_{H_2O}]}{[1 + K_{CO}P_{CO} + K_{H_2O}P_{H_2O}]^2} \quad (23)$$

If $K_{CO}P_{CO} \gg K_{H_2O}P_{H_2O}$, which can be justified on the ground that at any point of the reaction $P_{CO} \gg P_{H_2O}$, then reaction (23) is practically reduced to Eq. (20) thus explaining the peculiar kinetics of the rwgs reaction.

It is mentioned that the used catalyst, after approximately 60 h instream, was re-examined for its activity in an experimental set-up using $P_{CH_4} = P_{CO_2}$. A drop of activity/degree of conversion (x) around 10% for methane and 15% for carbon dioxide was observed, compared to the initial experimental data on the fresh catalyst. The drop was almost uniform in the whole temperature range. The results show (i) a

Table 3
The pairs of parameters k_1–K and k_2–K_{CO_2} as well as the correlation coefficients r^2 used for the fitting of Eqs. (20) and (21) to the experimental points in Fig. 7

T (K)	$R_{rwgs} \approx k_1(2xP_{CH_4})/[1 + K(2xP_{CH_4})]^2$			$R_{rwgs} \approx k_2 P_{CO_2}/[1 + K_{CO_2} P_{CO_2}]$		
	k_1	K	r^2	k_2	K_{CO_2}	r^2
813	7193 ± 696	223 ± 16	0.9756	48.3 ± 4.8	6.5 ± 1.0	0.9584
833	3649 ± 808	90 ± 13	0.9623	37.1 ± 1.5	2.0 ± 0.2	0.9944
853	1947 ± 301	40 ± 4	0.9466	52.3 ± 1.8	1.4 ± 0.1	0.9962
873	944 ± 138	20 ± 2	0.8733	42.9 ± 1.8	0.2 ± 0.1	0.9955
893	1349 ± 22	22 ± 4	0.8755	59.6 ± 3.6	0.3 ± 0.2	0.9922

middle catalyst deactivation takes place and (ii) that the rwgs reaction is suppressed more extensively compared to the reforming reaction. Further experiments are needed in order to clarify these effects.

A final comment is needed about the apparent reaction rates. An average value for both CH_4 and CO_2 conversion is around 10 $\mu mol/g_{cat}$ s (see Fig. 4). Since the solid contains 0.5% Pt, of which only 20% is located on the external surface of the oxidic support (EDS results) which is 12 m^2/g (BET results), the real reaction rate on the exposed noble metal is 10.10^3 $\mu mol/g_{Pt}$ s, e.g. higher by three orders of magnitude. So the strategy to improve the efficiency should be the development of alkaline supports of high surface area, due to internal pores with wall thickness equal to the size of Pt crystallites in order to take full advantage of all the dispersed particles of it.

5. Conclusions

(i) The kinetics of interconversion of methane with carbon dioxide over a 0.5%Pt/$SrTiO_3$ solid catalyst was studied in partial pressure range 0.083 atm $< P_{CH_4}, P_{CO_2} <$ 0.667 atm and in the temperature range 813–893 K.

(ii) The experimental data for the rate of methane conversion, R_{CH_4}, were fitted using the empirical equation $R_{CH_4} = k(P_{CH_4})^m(P_{CO_2})^n$ with $m \approx 1$ and $n \approx 0$. These results are explained using Langmuir–Hinshelwood kinetics and admitting that the reactants adsorbed on *distinct and discreet active sites* of the solids, namely the methane is weakly bound on the metallic and the carbon dioxide strongly adsorbed on the oxidic phase of the catalyst.

(iii) The rate of conversion of the carbon dioxide, R_{CO_2}, was considered to be the sum of the R_{CH_4} plus the rate of the reverse water gas shift reaction, $R_{rwgs.}$ The dependence of R_{rwgs} on the partial pressure of CO_2 appears similar to that of R_{CH_4}. On the contrary the dependence of R_{rwgs} on the partial pressure of H_2 shows a maximum which might be due to strong inhibition by the products CO and H_2O interacting and adsorbed strongly on the active surface.

Acknowledgements

We acknowledge financial support for A. Topalidis from the project PENED 2003 financed by the GSRT. We also acknowledge suggestions by the anonymous referees which resulted to substantial improvement of this work.

Appendix A. Supplementary data

Supplementary data associated with this article can be found, in the online version, at doi:10.1016/j.cattod.2007.04.015.

References

[1] F. Fischer, H. Tropsch, Brennstoff Chem. 3 (1928) 39.
[2] R.E. Hanneman, H. Vakil, R.H. Wentorf, in: Proceedings of Ninth Intersosiety Energy Conversion Engineering Conference, The American Society of Mechanical Engineers, 435, 1974.
[3] M.C. Bradford, M.A. Vannice, Catal. Rev. Sci. Eng. 41 (1999) 1.
[4] M.C. Bradford, M.A. Vannice, J. Catal. 173 (1998) 157.
[5] L.M. Aparicio, J. Catal. 165 (1997) 262.
[6] J.R. Rostrup-Nielsen, J.-H. Bak Hansen, J. Catal. 144 (1993) 38.
[7] Z. Zhang, X. Verykios, Appl. Catal. A: Gen. 138 (1996) 109.
[8] A.N.J. van Keulen, K. Seshan, J.H.B.J. Hoebink, J.R.H. Ross, J. Catal. 166 (1997) 306.
[9] J.H. Bitter, K. Seshan, J.A. Lercher, J. Catal. 171 (1997) 276.
[10] V. Tsipouriari, X. Verykios, Catal. Today 64 (2001) 83.
[11] A.A. Lemonidou, I.A. Vasalos, Appl. Catal. A: Gen. 228 (2002) 227.
[12] C. Ji, L. Gong, J. Zhang, K. Shi, J. Nat. Gas Chem. 12 (2003) 201.
[13] G. Goula, V. Kiousis, L. Nalbatian, I.V. Yentekakis, Solid State Ionics 177 (2006) 2119.
[14] (a) J. van Herle, Y. Membrez, O. Bucheli, J. Power Sources 127 (2004) 300;
(b) M. Hammad, D. Badarneh, K. Tanboub, Energy Convers. Manag. 40 (1999) 1463;
(c) J. Huang, R.J. Crookes, Fuel 77 (1998) 1793.
[15] (a) R. Hansen, in: G. Ertl, H. Knozinger, J. Weitkamp (Eds.), Handbook of Heterogeneous Catalysis, Wiley-VCH, 1997, p. 1856;
(b) V. Ponec, in: G. Ertl, H. Knozinger, J. Weitkamp (Eds.), Handbook of Heterogeneous Catalysis, Wiley-VCH, 1997, p. 1876.
[16] R.J. Farrauto, C.H. Bartolomew, Fundamentals of Industrial Catalytic Processes, Blackie Academic and Professional, 1997,, p. 357.
[17] T. van Herwijnen, W.A. de Jong, J. Catal. 63 (1980) 83.
[18] M.J.L. Gines, A.J. Marchi, C.R. Apesteguia, Appl. Catal. A: Gen. 154 (1997) 155.
[19] C.V. Ovesen, P. Stoltze, J.K. Norskov, C.T. Campbell, J. Catal. 134 (1992) 445.
[20] A.N. Topalidis, D.E. Petrakis, L.A. Loukatzikou, P. Falaras, P.J. Pomonis, Ninth Panhellenic Symposium on Catalysis, Lefkas, 6–7 October, 2006.
[21] V.C. Belessi, C.N. Costa, T.V. Bakas, T. Anastasiadou, A.M. Efstathiou, P.J. Pomonis, Catal. Today 59 (2000) 347.
[22] C.N. Costa, P.G. Savva, C. Andronikou, P.S. Lambrou, K. Polychronopoulou, V.C. Belessi, V.N. Stathopoulos, P.J. Pomonis, A.M. Efstathiou, J. Catal. 209 (2002) 456.